Current-Induced Vibrations of Submerged Tunnels

Susumu YOSHIHARA, Shozo TOYODA, Katta VENKATARAMANA, and Yorikazu AIKOU

(Received May 31, 1994)

Abstract

This paper deals with the current-induced motions of submerged tunnels i.e., instabilities that can arise for a submerged tunnel in a calm sea with a steady current. The dynamic response of smooth circular cylindrical models in unidirectional flow situations is investigated experimentally. The models were placed in a circulating water channel horizontally and normal to the direction of current flow. The two ends of the models were attached, using springs, to rigid supports. The traces of response vibrations for the inputs of current loading were recorded using video camera. The time histories of displacements along the horizontal and vertical direction were deduced from this data. Then, by Fourier analysis, the dominant frequencies of vibration were identified. The Strouhal number, which is a function of eddy-shedding frequency, was computed and is shown against Reynold's number.

1. Introduction

Japan is surrounded by sea on all sides and consists of four main islands and hundreds of smaller islands. The main islands are now well-connected by bridges over the sea or tunnels on the bottom of the sea. But as the separation length as well as the depth increase, these types of connections are becoming extremely difficult for construction both from technical and economical viewpoints. As the ocean development grows, it has become necessary to study alternate forms of channel-crossing concepts. In this regard, the under-water channel or the so-called submerged floating tunnels are attracting wide interest in the engineering and the academic circles. Japan Society of Civil Engineers (JSCE) has a subcommittee which is currently investigating the feasibility of such tunnels and several articles related to these topics appeared last year in the Journal of JSCE under the general heading 'Concepts of Transport Systems in the Sea' (Refs. 1 to 3). It seems that the submerged tunnel concept may become a major part of the infrastructure of the 21st century.

A submerged tunnel is a structure somewhere in between a conventional bridge over the sea and a tunnel at the sea bottom. It may be constructed using steel or concrete or composite of steel and concrete. The submerged tunnel is neither on the sea surface nor on the sea bottom but will be located as a floating structure inside the sea. The tunnel has buoyancy force which is utilized to neutralize the dead loads and the live loads as much as possible. The section of the tunnel can be divided into a number of segments for several uses simultaneously, such as for the transportation of vehicles and railways, for carrying cables, for carrying industrial and urban waste for treatment/disposal and so on.

Until now the concepts of submerged tunnel were put forward for a few cases such as

Gibraltar Sea crossing, but not persued further. There is not a single case of submerged tunnel in use till today. Therefore extensive research is required in this direction.

The writers investigated (Ref. 4) earlier experimentally the fluid forces due to current flow on submerged tunnel models. In the present paper, the vibrations of those submerged tunnels are studied further. The models have the same diameter but are smaller in length than the previous case and are held in position using springs. Thus they are susceptible to large displacements.

2. Experimental setup

Experiments were carried out in the circulating water channel of the Faculty of Fisheries of Kagoshima University. The measuring section of this channel is 6 m in length, 2 m in width and 1 m in depth with a maximum water velocity of 2 m/sec. Hollow cylindrical pipes made of poly-vinyl chloride were used as experimental models. The diameter of the model is 75mm and the length is 200mm. For recording the movement of the pipe accurately, acryl plates of 220mm in diameter were securely attached to the two ends of a rod passing through the center-line of the model. On one of the plates, eight points were marked at equal distances along the radial direction using black vinyl tapes. The vibration of these points were recorded later. The model was held in its position by means of springs at the ends. Figure 1 shows the schematic diagram of the model. Figure 2 is a photo of the model.

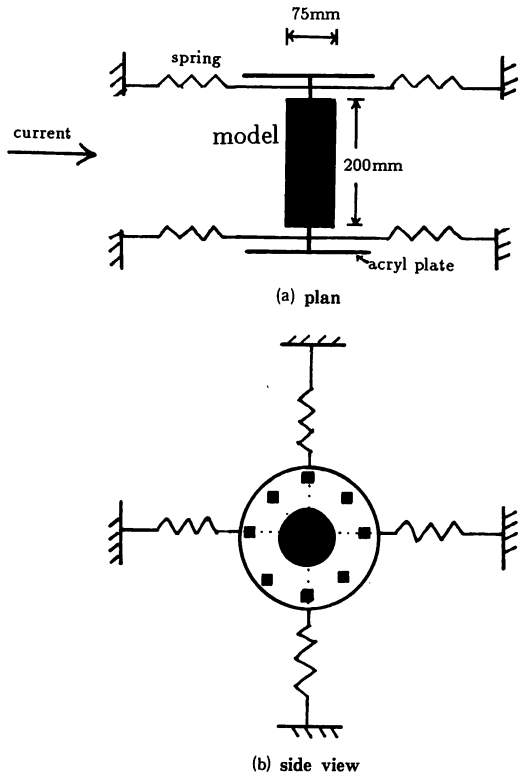

Figure 1 Schematic diagram of model.

Since the width of the circulating water channel is very much larger than the dimension of the model, a new flume, made of acryl plates, of length 2.5 m, height 1 m and width 200mm (i.e., equal to the length of the model) was constructed to generate accurate two-dimensional flow conditions. Figure 3 is a photo of this flume. The model was set at the center and held in position by means of four springs at either ends, securely fastened as shown. The springs are attached such that two springs are in horizontal direction and the other two springs are in the vertical direction. The angle between any two successive springs is 90°.

The flume, with the model placed inside, was lowered into the measuring section of the circulating water channel and placed at the center. Figure 4 is a photo of the model inside the flume and placed in the water channel. The model was sagging in Figure 3 due to self weight. But in Figure 4, due to buoyancy action, it is held with approximately equal force by the four springs at each end.

Figures 5 and 6 respectively show the steady responses of the model for a low and a high value of current velocity. Also, two types of springs were used for securing the model. One type was a very soft spring and the other type was relatively a rigid spring. The stiffness of the rigid spring was about four times the stiffness of the soft spring. The system consisting of soft springs is referred to as Model 1 in this paper and that consisting of rigid springs as

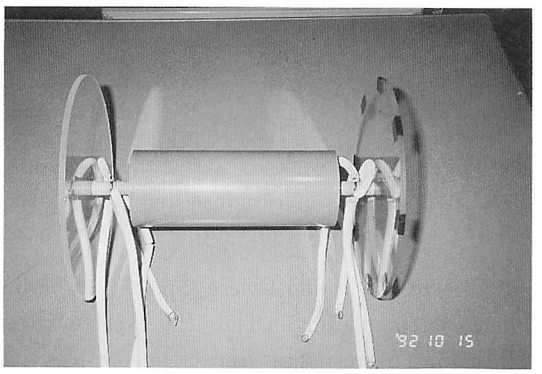

Figure 2 Photo of a model.

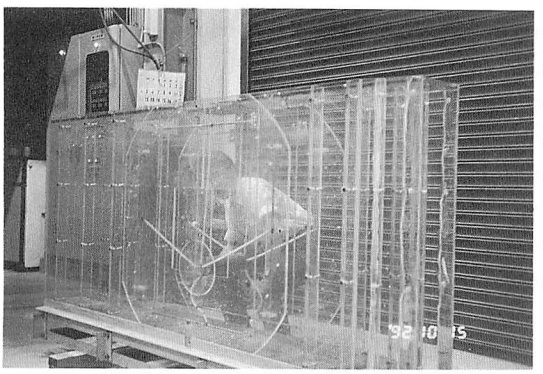

Figure 3 Flume with the model set inside.

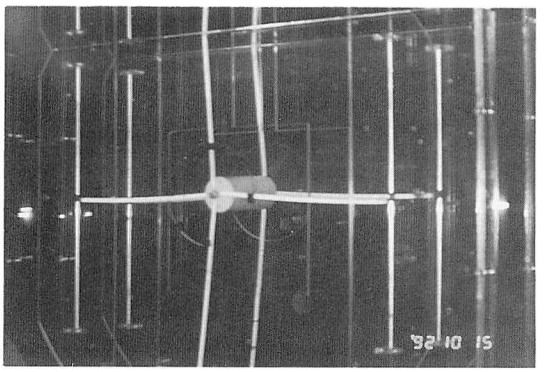

Figure 4 Model inside the water channel with no current.

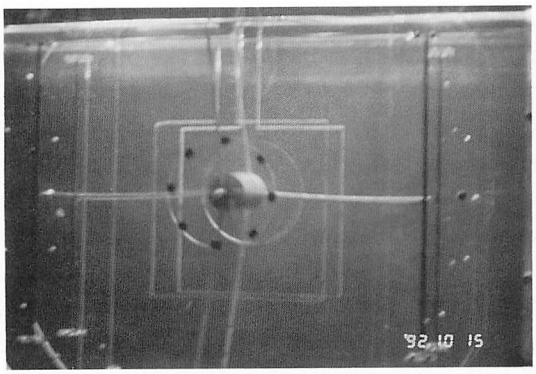

Figure 5 Model inside the water channel with slow current.

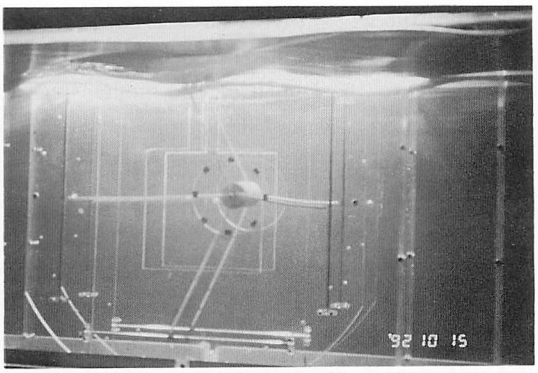

Figure 6 Model inside the water channel with fast current.

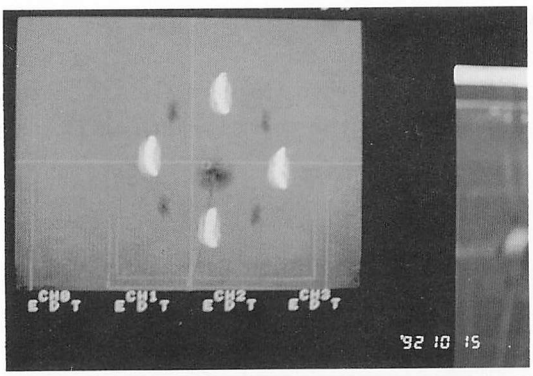

Figure 7 Traces of response displacements displayed on computer monitor.

Model 2. The response displacements of Model 1 were expected to be larger than that of Model 2 for the same values of input current loadings. Thus the experiment allowed the studies to be undertaken on different situations of response vibrations for identical fluid loadings.

Firstly free vibration experiments were conducted by giving an initial displacement to the model and then releasing it from that displaced position. The decaying vibration pattern was recorded using video camera. Then forced vibration experiments were conducted for various inputs of current flow. When the response vibration of the model was fairly steady under current flow, its movement was recorded using video camera i.e., the traces of the points marked on the acryl plates on the side of the model were recorded. Figure 7 shows the traces of four points on the display monitor of a computer. Using the video tracker, each of these traces was divided into horizontal and vertical components consisting of 2048 discrete data, the time step of digitization being 1/30 second. The time history of the mean vibration of the center of gravity of the model along horizontal (or vertical) direction was obtained by computing the average of the four traces along the horizontal (or vertical) direction. Then, the mean value of the displacement, of the center of gravity of the model, along horizontal (or vertical) direction was computed by averaging the 2048 values of the displacements.

3. Results

Figure 8 shows the response curves of free vibration experiments. The values of natural frequencies are 0.75Hz (i.e., natural period $T_0=1.33$s) for Model 1 and 1.55Hz (i.e., $T_0=0.65$s) for Model 2. The damping ratios are 4.9% for Model 1 and 4.1% for Model 2. Figure 9 shows the Fourier amplitudes of free vibration response obtained by FFT analysis of time histories of response data.

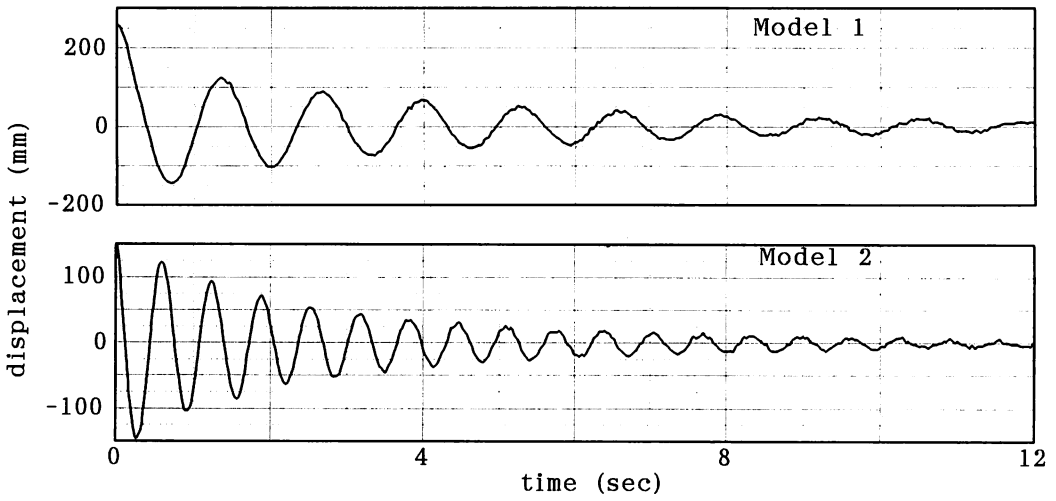

Figure 8 Time histories of free vibration response.

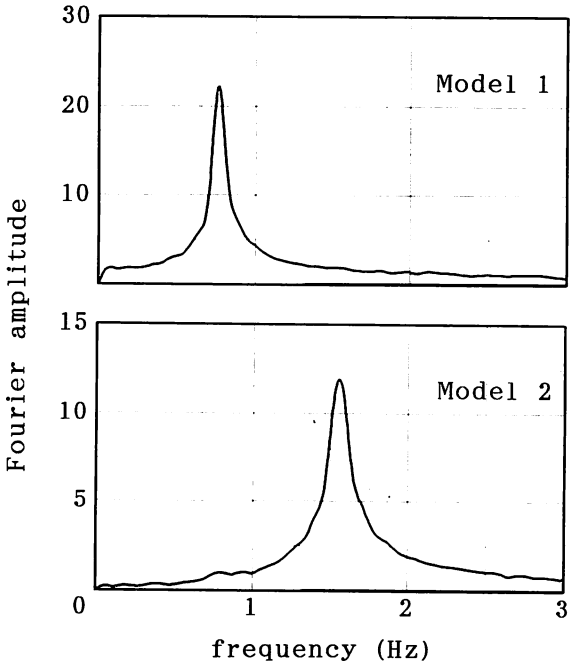

Figure 9 Fourier amplitudes of free vibration response.

Forced vibration experiments were conducted for current velocities ranging from 0.1 m/s to 1.1 m/s for Model 1 and 0.1 m/s to 1.4 m/s for Model 2 at 0.1 m/s intervals. Figures 10 and 11 show the examples of traces of response displacement of the center of gravity of Model 1 and Model 2 respectively for the duration of about 60 seconds. The numbers inside the figures indicate the current velocities in meters per second. The time histories of the components of

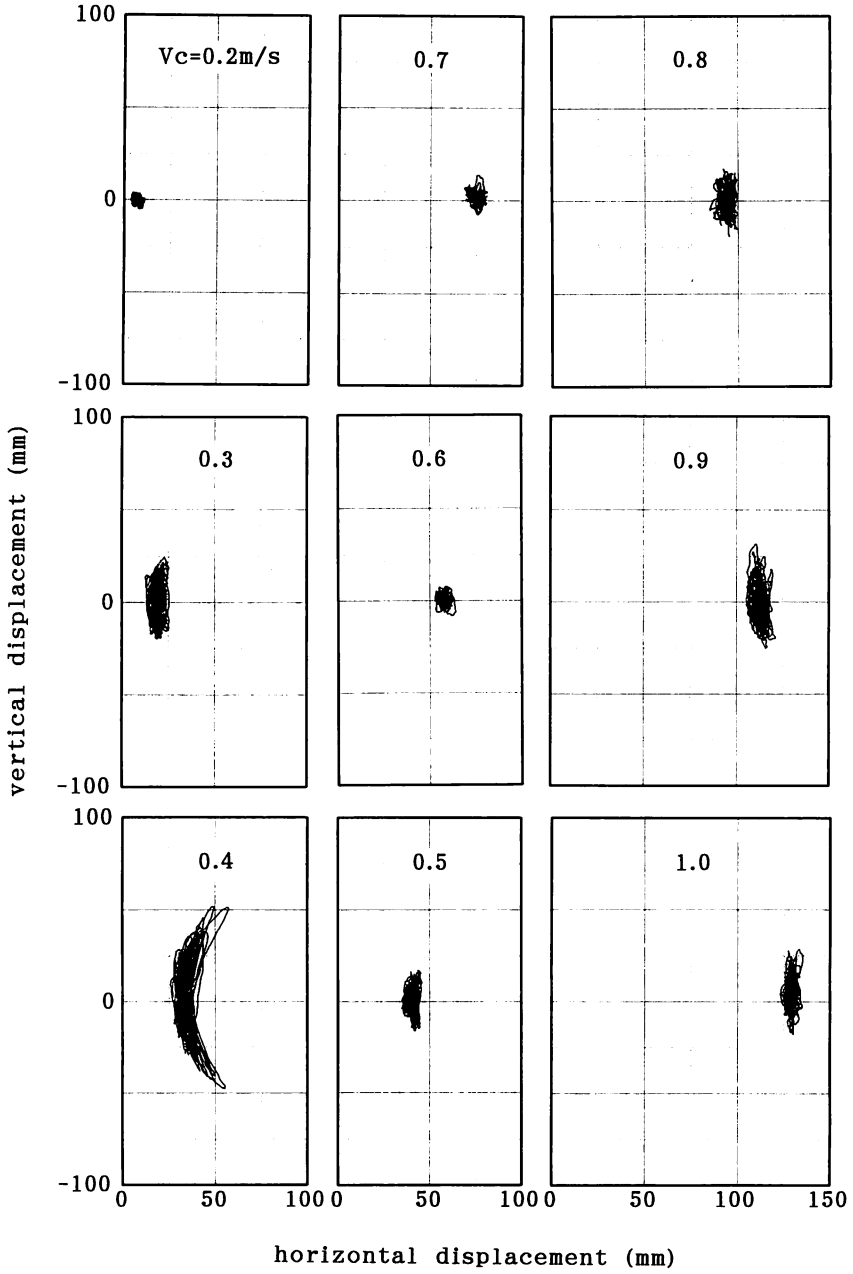

Figure 10 Traces of response displacements of Model 1 for different current velocities.

the major traces in the horizontal and vertical direction are shown in Figures 12 and 13. In the figures, the thin line shows the horizontal component whereas the thick line shows the vertical component of response displacement of the models. The horizontal component of displacement increases with the increase in current velocity as expected due to the increase in fluid drag force. But their temporal variation is relatively small for any current velocity.

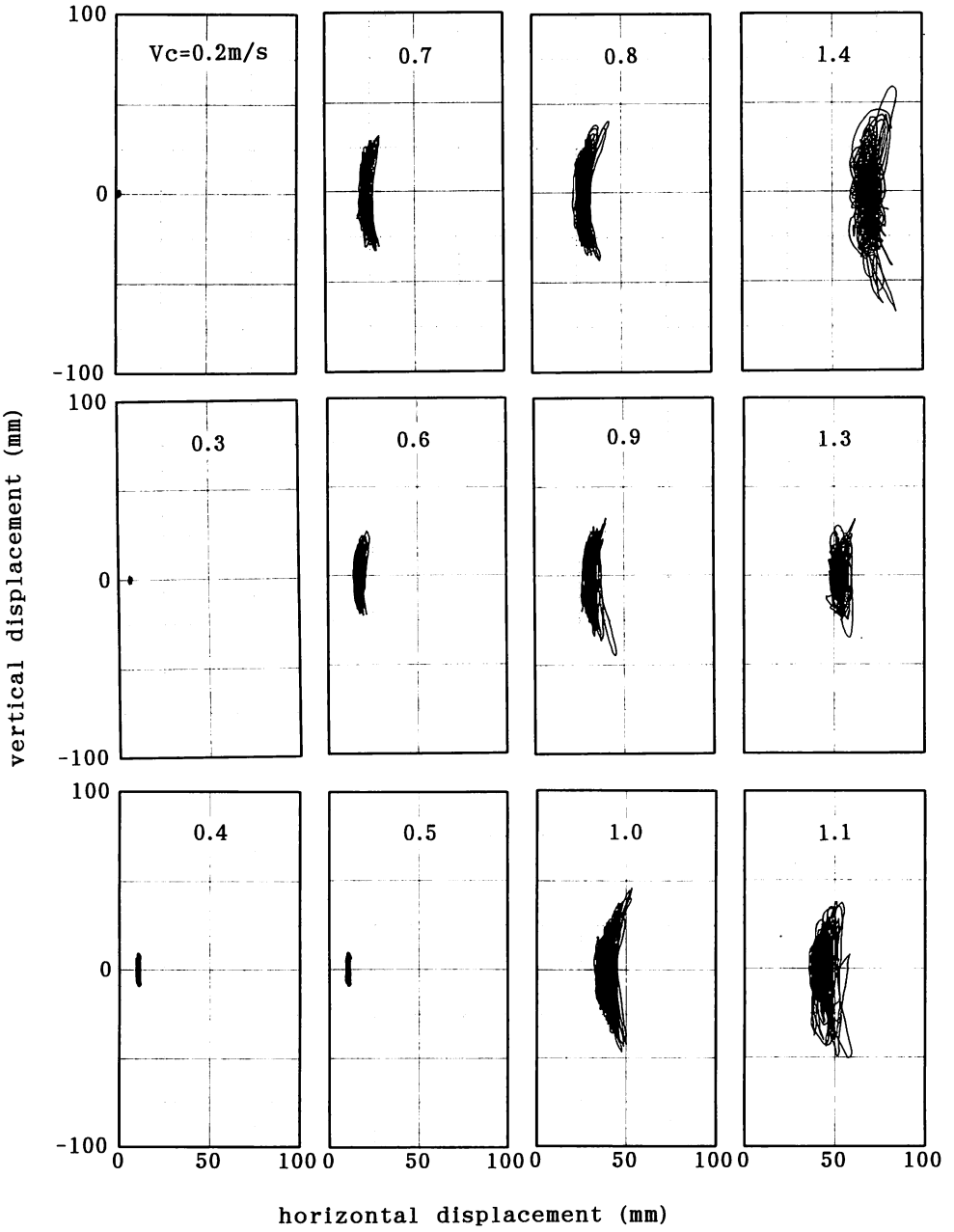

Figure 11 Traces of response displacements of Model 2 for different current velocities.

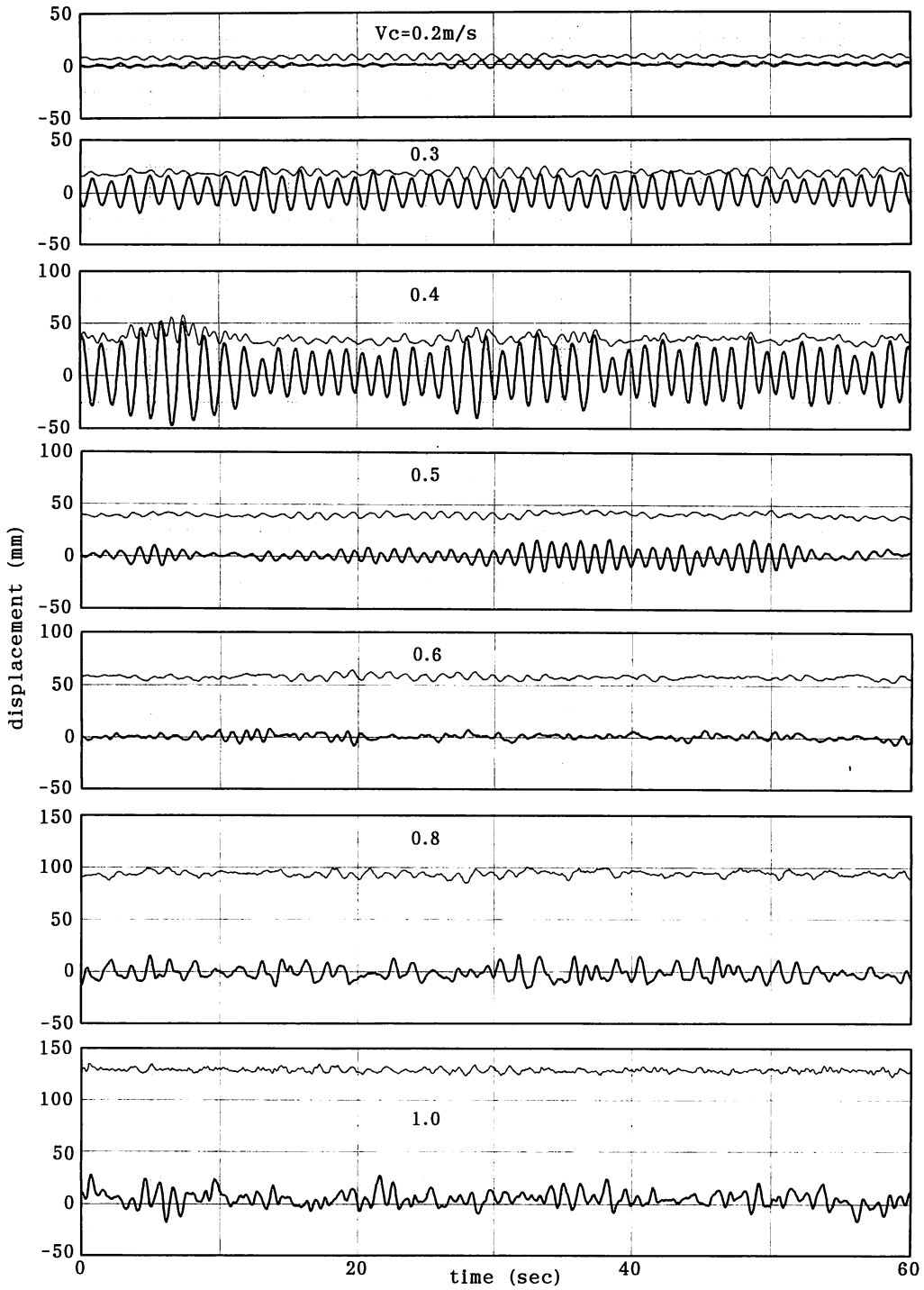

Figure 12 Time histories of response displacements of Model 1.
(—— horizontal component; ——— vertical component)

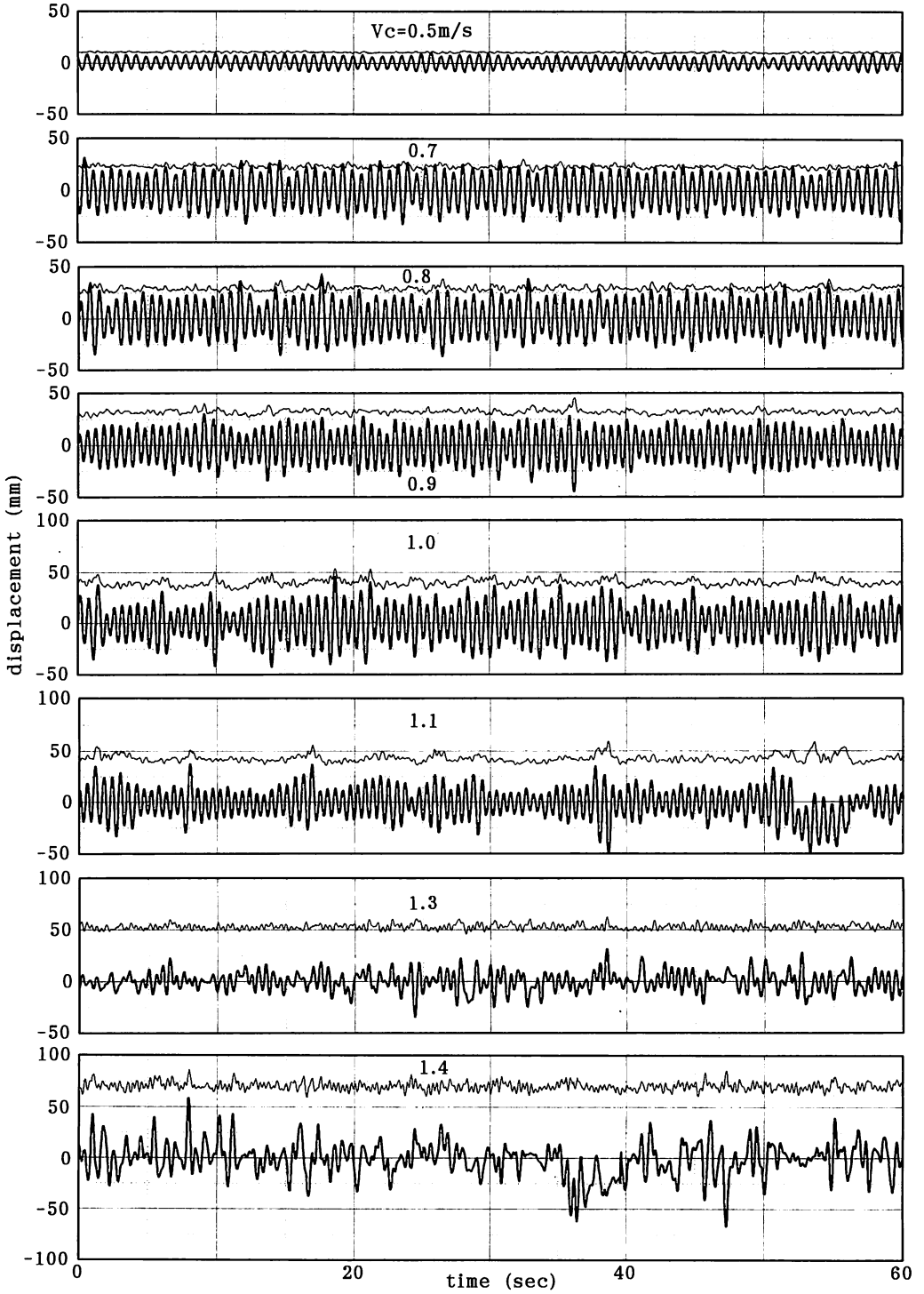

Figure 13 Time histories of response displacements of Model 2.
(—— horizontal component; ——— vertical component)

The vertical component of displacement, which is caused by fluid lift force (due to the eddy-shedding phenomenon), increases initially with the increase in current velocity. Largest values are observed at current velocities of 0.4m/s for Model 1 which may be due to the proximity of the eddy-shedding frequency to the natural frequency of the model. The vibration is approximately periodic when we look at the periods of vibration. This is due to the generation of a regular number of eddies caused by wake. On the other hand, the amplitude of displacement is clearly random due to interaction between the current flow and the vibrating model. Thus, the vibration of the model is fairly regular from the point of view of period of vibration, but, is clearly random as far as the amplitude of displacement is concerned. Even if there is a slight variation in the pattern of generation of eddies due to the movement of the model, the fluid-structure interaction causes the model to vibrate with different amplitude in the following cycle.

The motion becomes chaotic with random period and random amplitude of vibration as the flow becomes fast i.e., as the current velocity increases and the flow is more and more turbulent. For Model 1, the occurrence of this behaviour is observed for current velocities above 0.6m/s whereas for Model 2 for current velocities above 1.2m/s. Although the flow is said to become turbulent when the Reynold's number exceeds a certain value (which is the same for the two models because their diameter are the same), the motion of the two models become chaotic at different current velocities. This is due to the fact that the degree of vertical displacement varies depending on the lift force which in turn depends on the eddy-shedding frequency. This eddy-shedding frequency is a function of not only the fluid velocity (or Reynold's number) but also the extent of fluid-structure interaction. Fluid-structure interaction itself depends on multiple factors such as the natural frequency of the structure, eddy-shedding frequency, parameters of the kinematics of the flow field and so on.

Figure 14(a) shows the mean response displacements of the models. The mean values of the horizontal and vertical components of the displacements are plotted againt current velocities. Note that each value of the displacement corresponds to the average value of the displacement data for about 68-second duration. The horizontal displacement increases sharply for Model 1 than for Model 2 with the increase in current velocity because this structure is more flexible and more susceptible to undergo displacement. In general, the horizontal displacements of both the models grow with the increase in current velocity due to larger fluid drag forces. The average values of vertical displacements are nearly zero for both the models, but this does not imply the absence of lift forces. Figure 14(b) shows the rms displacements of the models. The values for the vertical component show a peak for certain values of current velocity which may be due to occurrence of regular eddy-shedding with their frequency being equal to or nearer to the natural frequency of the model.

For steady flows past structures, the main measure of the frequency of lift forces or the eddy-shedding frequency is the Strouhal number S which is a function of the eddy-shedding frequency and is defined as $S=Df/Vc$ where D is the diameter of the model, f is the eddy-shedding frequency and Vc is the current velocity. In the present study, the time histories of components of displacements in the vertical direction were analyzed using Fast Fourier Transform and frequencies corresponding to maximum amplitudes were located. Assuming that these correspond to eddy-shedding frequencies at each current velocity, Strouhal number was calculated. Figures

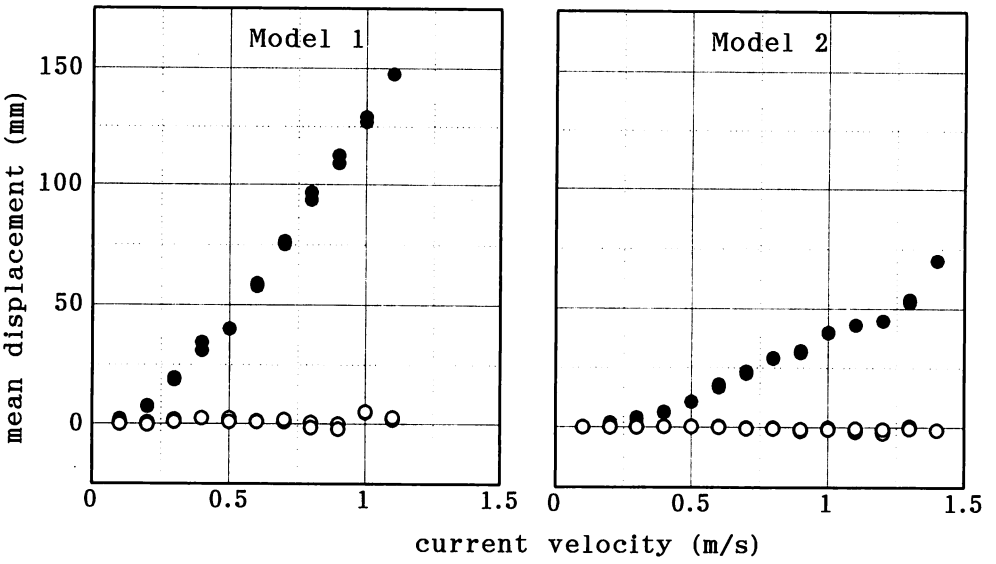

(a) mean response displacements

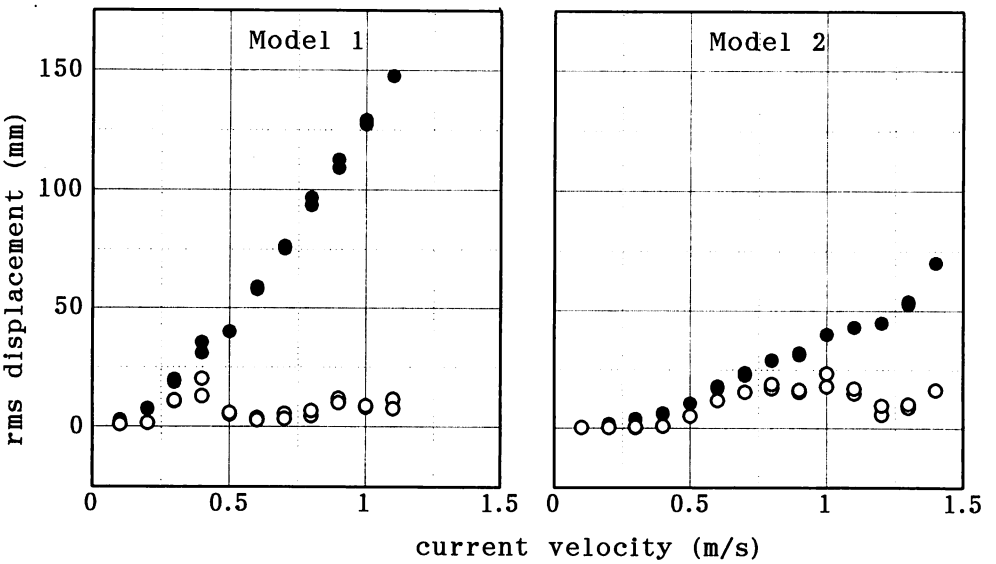

(b) rms response displacements

Figure 14 Mean and rms response displacements.
(● horizontal component; ○ vertical component)

15 to 17 show the results of FFT analysis. The Fourier amplitudes are plotted against the frequencies in Figure 15 for Model 1 and in Figure 16 for Model 2. Figures 17(a) and (b) show the results for the case of long-pipe model (7.5cm in diameter and 1.8m in length) discussed in our earlier paper (Ref. 4), where the time histories of vertical strains were analyzed by FFT.

Figure 18 shows the Strouhal number plotted as a function of Reynold's number. The higher is the value of Reynold's number, of course, the faster is the current flow. The results

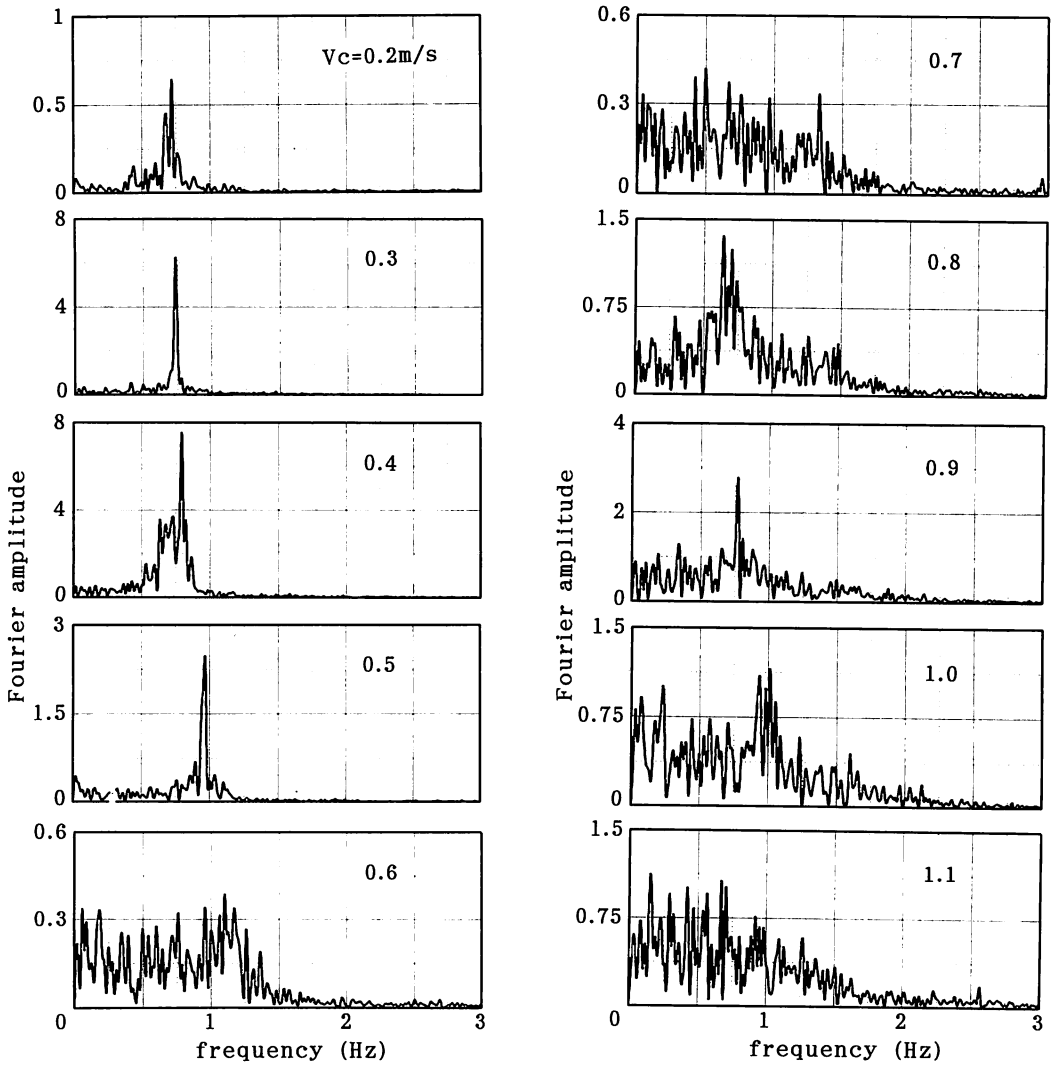

Figure 15 Fourier amplitudes of vertical displacements of Model 1.
(results of FFT analysis)

for Model 1 and Model 2 are compared with their equivalent values for the case of the long-pipe model. The end conditions of the long pipe were different from the present models and the long-pipe model was almost stationary. The values of the Strouhal number for the long pipe are relatively constant for the range of the Reynold's number indicating regular shedding. In the present experiments, the models are quite flexible and are susceptible to undergo vibration. It may be possible that additional eddies may be triggered by the vibration of the model, which will be produced at or near the resonant frequency of the model and the lift forces may be several times higher than those anticipated on equivalent stationary structures (Ref. 5, 6). Therefore the patterns of Strouhal numbers are quite different for the vibrating models of the present experiment than those for the long-pipe model of our earlier study.

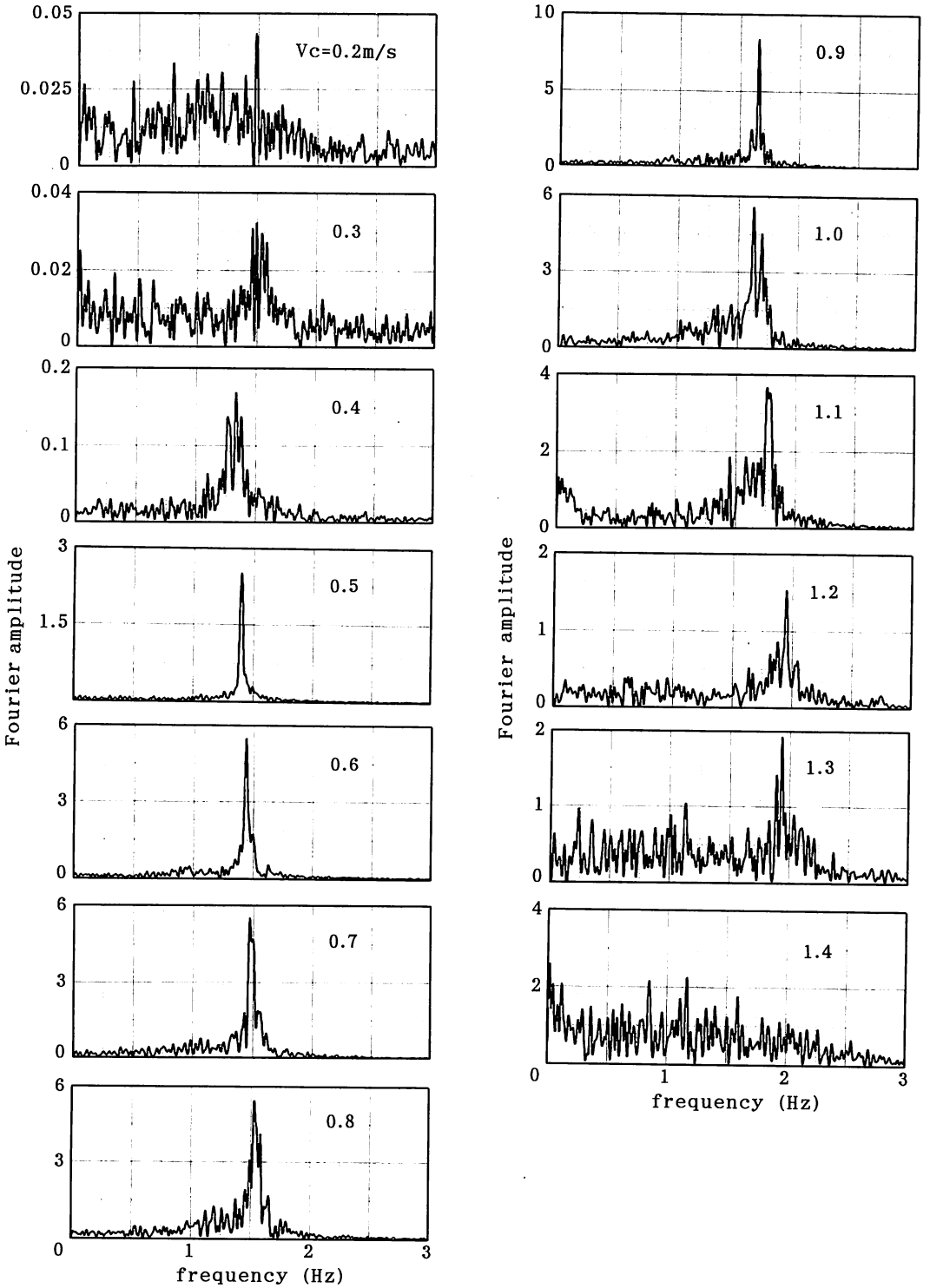

Figure 16 Fourier amplitudes of vertical displacements of Model 2.

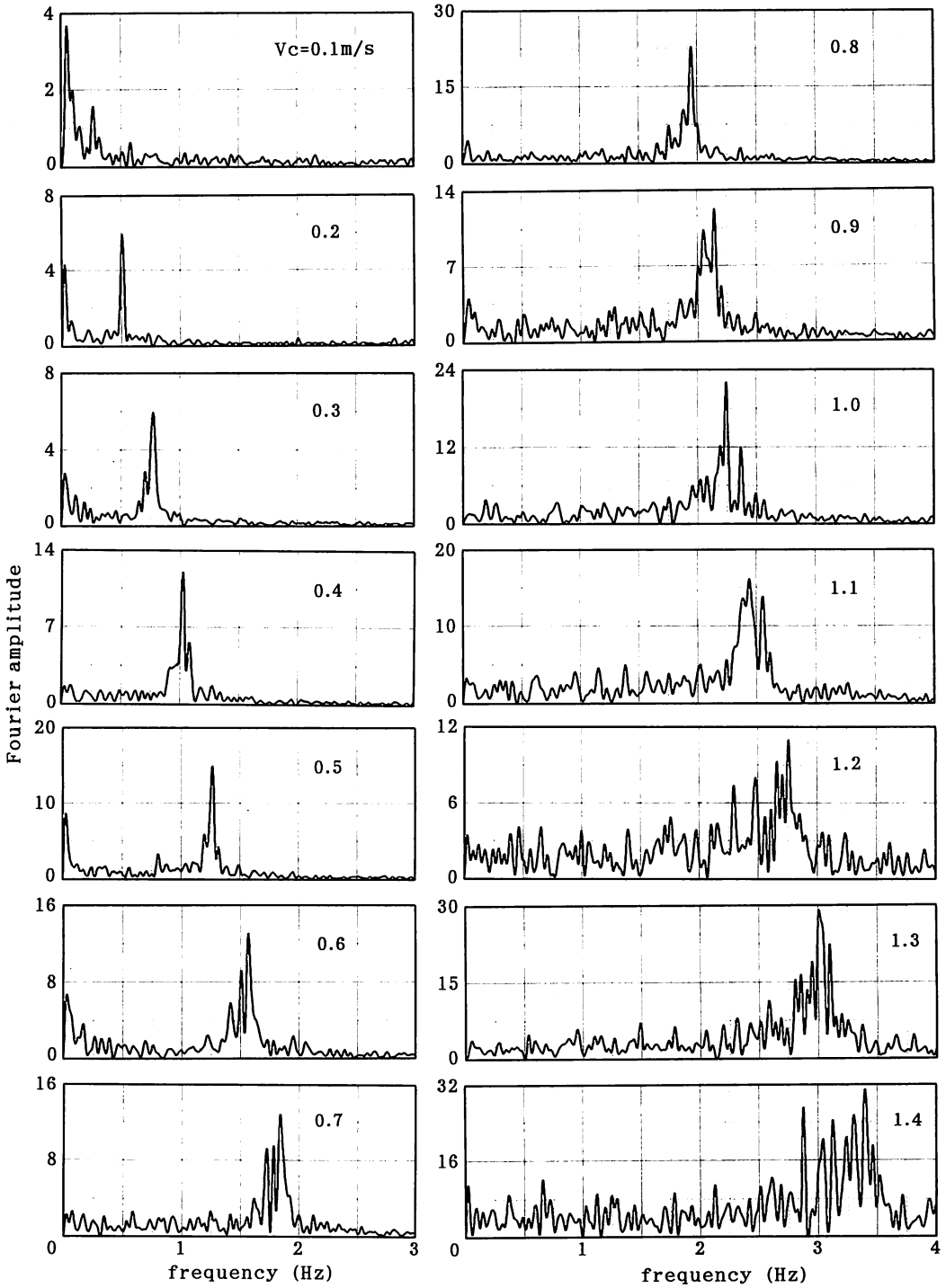

Figure 17 (a) Fourier amplitudes of vertical strains of long-pipe model.

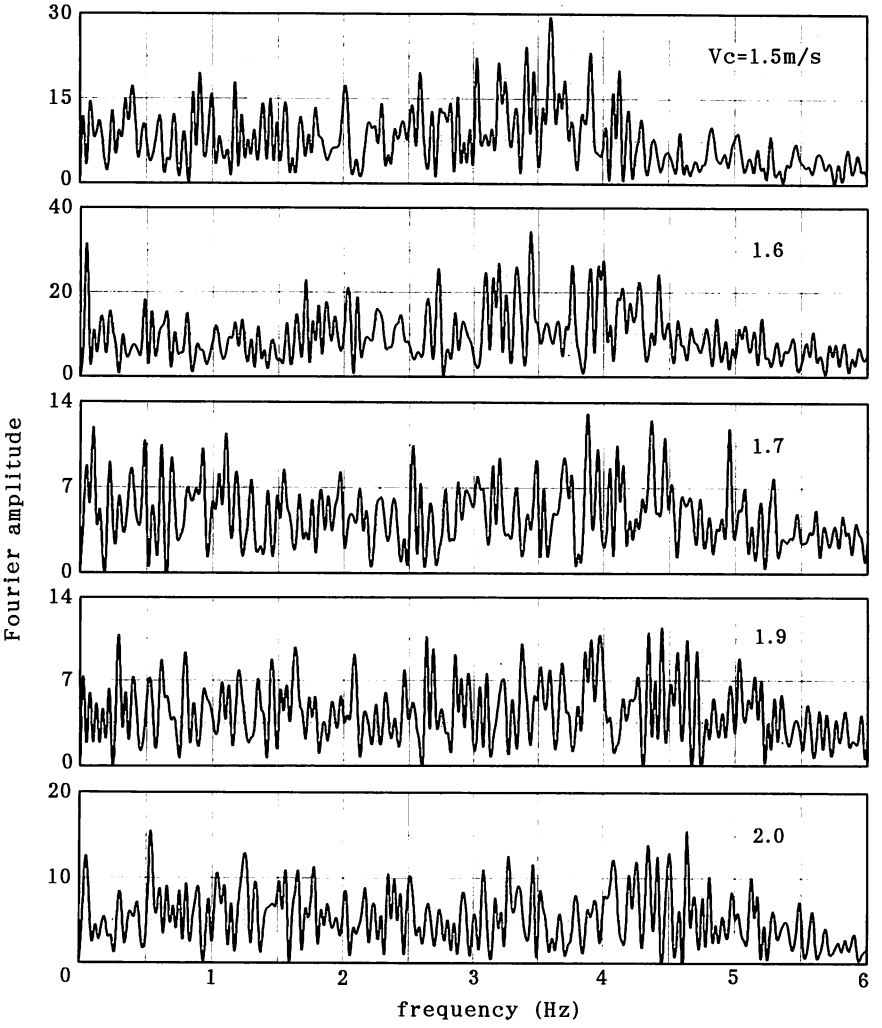

Figure 17 (b) **Fourier amplitudes of vertical strains of long-pipe model.**

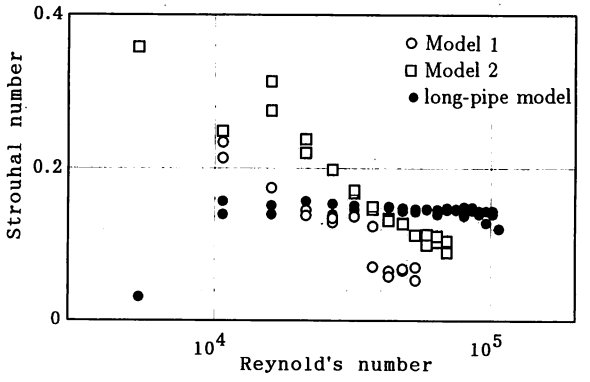

Figure 18 Values of Strouhal number.

4. Conclusions

A laboratory study on the vibrations of submerged tunnel models in steady current flow has been carried out. It is found that the horizontal components of response displacements generally increase with flow velocity, as expected, due to the action of higher fluid drag forces. The variation of lift force is more complex and is significantly affected by the eddies and other forms of turbulence around the models and due to fluid-structure interaction effects. When the natural frequency of the model is nearer to the eddy-shedding frequency, the values of vertical components of displacements, and hence the lift forces are maximum. Also for larger current velocities, the flow becomes chaotic around the models with irregular eddy-shedding and the models show patterns of severe random vibration. From an engineering standpoint, the oscillatory vertical displacement due to lift force may be of more practical importance than the drag, especially if a hydroelastic resonance occurs between the eddy-shedding frequency and a structural mode of vibration of submerged tunnel.

There are no cases so far of actual construction of submerged tunnels. Therefore a great deal of theoretical and experimental investigations are necessary before the actual execution of the project. In this regard the present research has examined some of the possible problems that can arise for submerged tunnels. As a next step, writers intend to extend the study for the wave-induced vibrations.

Acknowledgements

The experiments were carried out in the circulating water channel of the Faculty of Fisheries of Kagoshima University. Mr K. Shimazumi and Mr M. Terawaki, undergraduate students, helped in the laboratory experiments.

References

1. Yoshimura, J. and Mikami, T. (1993), Submerged floating channels, *J. of JSCE*, 78 (8), pp. 32–33 (in Japanese).
2. Hamada, T. *et al.* (1993), The channel-crossing submerged tube concept, *J. of JSCE*, 78 (8), pp. 34–35 (in Japanese).
3. Ohta, T. (1993), The marine Express concept, *J. of JSCE*, 78 (8), pp. 36–37 (in Japanese).
4. Yoshihara, S. *et al.* (1993), Hydrodynamics of Ocean Pipelines, *The Research Reports of the Faculty of Engineering*, Kagoshima University, No. 35, pp. 143–153.
5. Brebbia, C. A. and Walker, S. (1979), Dynamic Analysis of Offshore Structures, Newness-Butterworths, London.
6. Newman, J. N. (1992), Marine Hydrodynamics, The MIT Press.